Eur J Nucl Med Mol Imaging (2010) 37:575–588
DOI 10.1007/s00259-009-1293-8

ORIGINAL ARTICLE

Quantitative analysis of [^{18}F]FDDNP PET using subcortical white matter as reference region

Koon-Pong Wong · Mirwais Wardak · Weber Shao · Magnus Dahlbom · Vladimir Kepe · Jie Liu · Nagichettiar Satyamurthy · Gary W. Small · Jorge R. Barrio · Sung-Cheng Huang

Received: 8 July 2009 / Accepted: 25 September 2009 / Published online: 31 October 2009

Abstract
Purpose Subcortical white matter is known to be relatively unaffected by amyloid deposition in Alzheimer's disease (AD). We investigated the use of subcortical white matter as a reference region to quantify [^{18}F]FDDNP binding in the human brain.

Methods Dynamic [^{18}F]FDDNP PET studies were performed on 7 control subjects and 12 AD patients. Population efflux rate constants (k_2') from subcortical white matter (centrum semiovale) and cerebellar cortex were derived by a simplified reference tissue modeling approach incorporating physiological constraints. Regional distribution volume ratio (DVR) estimates were derived using Logan and simplified reference tissue approaches, with either subcortical white matter or cerebellum as reference input. Discriminant analysis with cross-validation was performed to classify control subjects and AD patients.
Results The population estimates of k_2' in subcortical white matter did not differ significantly between control subjects and AD patients but the variability of individual estimates of k_2' determined in white matter was lower than that in cerebellum. Logan DVR showed dependence on the efflux rate constant in white matter. The DVR estimates in the frontal, parietal, posterior cingulate, and temporal cortices were significantly higher in the AD group ($p<0.01$). Incorporating all these regional DVR estimates as predictor variables in discriminant analysis yielded accurate classification of control subjects and AD patients with high sensitivity and specificity, and the results agreed well with those using the cerebellum as the reference region.
Conclusion Subcortical white matter can be used as a reference region for quantitative analysis of [^{18}F]FDDNP with the Logan method which allows more accurate and less biased binding estimates, but a population efflux rate constant has to be determined a priori.

Keywords Alzheimer's disease · [^{18}F]FDDNP · Reference tissue modeling · Subcortical white matter · Discriminant analysis

K.-P. Wong (✉) · M. Wardak · W. Shao · M. Dahlbom · V. Kepe · J. Liu · N. Satyamurthy · J. R. Barrio · S.-C. Huang
Department of Molecular and Medical Pharmacology,
David Geffen School of Medicine at UCLA,
Rm. B2-085E CHS, 10833 Le Conte Avenue,
Los Angeles, CA 90095, USA
e-mail: kpwong@ucla.edu

M. Wardak · S.-C. Huang
Department of Biomathematics,
David Geffen School of Medicine at UCLA,
Los Angeles, CA, USA

G. W. Small
Department of Psychiatry and Biobehavioral Sciences,
David Geffen School of Medicine at UCLA,
Los Angeles, CA, USA

G. W. Small
Semel Institute for Neuroscience and Human Behavior,
David Geffen School of Medicine at UCLA,
Los Angeles, CA, USA

G. W. Small
UCLA Center on Aging,
David Geffen School of Medicine at UCLA,
Los Angeles, CA, USA

G. W. Small
Mary S. Easton Center for Alzheimer's Disease Research,
Los Angeles, CA, USA

Introduction

Positron emission tomography (PET) imaging with 2-(1-{6-[(2-[^{18}F]fluoroethyl)(methyl)amino]-2-naphthyl}ethylidene)malononitrile ([^{18}F]FDDNP) has been found useful to differentiate Alzheimer's disease (AD) from mild cognitive impairment (MCI) and normal aging [1, 2], and to show prion protein amyloid accumulation in the brain of patients with Gerstmann-Sträussler-Scheinker (GSS) disease [3]. [^{18}F]FDDNP is a hydrophobic molecular probe that crosses the blood–brain barrier rapidly and shows excellent in vitro fluorescence visualization of and high binding affinity for the rigid fibrillar aggregates of width 4–20 nm, the main components of β-amyloid plaques and neurofibrillary tangles that are the characteristic neuropathological hallmark of AD [4, 5]. [^{18}F]FDDNP is currently the only PET molecular imaging probe known to label both amyloid and tangles in the living brain. The main potential for [^{18}F]FDDNP is to use it to follow disease progression and treatment response, as other tracers appear not suitable for these purposes, i.e., they behave as on/off tracers with no correlation with severity of disease.

A number of simplified and parametric methods have been evaluated [6, 7] and validated against the "gold standard" of kinetic analysis with metabolite-corrected arterial input function [8]. Quantification of [^{18}F]FDDNP PET data has been primarily based on distribution volume ratio (DVR) using Logan graphical analysis [9], due to its robustness and simplicity as compared to other simplified reference tissue modeling methods with the cerebellum as reference input [6]. The use of the cerebellum as the reference region is based on an assumption that its amyloid deposition is negligible. However, post-mortem studies have shown that a diffuse type of senile plaques exists in the cerebellum of some AD patients [10, 11]. Also, in patients with GSS, prion protein is known to accumulate in the cerebellum [12]. The use of the cerebellum as the reference region in these cases and in other diseases where there is significant amyloid deposition in the cerebellum is therefore inadequate. Thus, there is a need to explore alternative regions which are not affected by the pathology of the disease.

Subcortical white matter has been demonstrated to be relatively unaffected by amyloid deposition [13], and has been used as a reference region for [^{18}F]FDDNP studies in GSS patients [3]. In this study, the use of subcortical white matter as the reference region to quantify [^{18}F]FDDNP binding in the human brain was investigated systematically. Using the white matter as the reference region, the transport properties of [^{18}F]FDDNP in control subjects and AD patients, error analysis of the Logan method, and classification performance in discriminating control subjects from AD patients were evaluated, and the results were compared to those obtained using the cerebellum as the reference region. Differences in nonspecific binding between the cerebellum and the subcortical white matter were also assessed in this population. The introduction of the use of the white matter region as a reference tissue in this work is an important issue since it is not only specific to [^{18}F]FDDNP, but is also relevant to all amyloid and neuroreceptor imaging studies when no appropriate cortical reference region can be used due to the presence of specific binding.

Materials and methods

Subjects

Seven control subjects (four men, three women; age 70±9 years; MMSE score 29±1) and 12 AD patients (six men, six women; age 74±8 years; MMSE score 18±7) were selected from our existing subject population [1], based on the criteria that the subjects were aged 60 years or above and the same imaging protocol and scanner was used. All subjects underwent thorough screening laboratory testing, neurological and neuropsychological evaluation with Mini Mental State Examination [14], and structural imaging scanning to rule out other possible causes of cognitive impairment [1]. All AD patients met the standard diagnostic criteria of memory impairment and had progressive impairment of memory and impairment in at least one other cognitive domain [15]. Control subjects had normal cognitive functioning for their age and did not meet the criteria for MCI or AD. Written informed consent was obtained from all subjects or from a family member or guardian of impaired AD patients, in accordance with procedures of the Human Subjects Protection Committee of the University of California, Los Angeles.

[^{18}F]FDDNP PET imaging

Synthesis of [^{18}F]FDDNP has been described previously [16]. Dynamic [^{18}F]FDDNP PET data were acquired on an ECAT EXACT HR+ scanner (Siemens/CTI, Knoxville, TN). Transmission scans were acquired with a set of ^{68}Ge rotating rod sources for 20 min to allow subsequent attenuation correction and movement correction. Immediately after injection of 382.2±27.6 MBq (mean±SD) of [^{18}F]FDDNP through an indwelling venous catheter, dynamic PET scans were acquired in 3-D acquisition mode for 125 min with a scanning protocol of 6×30 s, 4×3 min, 5×10 min, and 3×20 min. Raw data were reconstructed using filtered back-projection (Hann filter cutoff at 0.3 of the Nyquist frequency), with correction for randoms, dead-time, scatter, normalization, photon attenuation and decay. An image-based head movement correction procedure was applied to

correct for misalignments between transmission and emission scans and between emission image frames [17].

Images were analyzed with CAPP software (Siemens/CTI, Knoxville, TN) on Sun workstations (Sun Microsystems, Mountain View, CA). For each subject, a summed image of the first 6 min of emission data was generated and regions of interest (ROIs) were then manually drawn on the summed image for the cerebellum, centrum semiovale (subcortical white matter), frontal, parietal, posterior cingulate, medial temporal, and lateral temporal regions. The summed image was used because it reflects initial flow-dependent activity distributions that enhance detection of distribution boundaries and cortical regions. The ROIs were projected onto the dynamic images at all time frames to calculate the associated tissue time–activity curves (TACs).

Kinetic analysis

Logan graphical analysis

The equation used in the Logan graphical analysis to determine the DVR of a reversible system using a TAC derived from a reference region is given by [9]:

$$\frac{\int_0^t C_T(\tau)d\tau}{C_T(t)} = \mathrm{DVR}\frac{\int_0^t C_R(\tau)d\tau + C_R(t)/\overline{k_2'}}{C_T(t)} + b \qquad (1)$$

where $C_R(t)$ and $C_T(t)$ denote, respectively, the activity concentration measured by PET in the reference region and the target region, and $\overline{k_2'}$ (in min^{-1}) is a population-averaged tissue-to-plasma efflux constant (from the reference region) which must be assumed or determined a priori. The y-intercept, b, includes a term which accounts for time-dependent differences between regions by using $\overline{k_2'}$ in place of the individual efflux rate k_2' (in min^{-1}) from the reference region [9]. The DVR can be determined as the slope of the linear portion ($t>t^*$) of a plot of $\left(\int_0^t C_R(\tau)d\tau + C_R(t)/\overline{k_2'}\right)/C_T(t)$ versus $\int_0^t C_T(\tau)d\tau/C_T(t)$. In this study, a bilinear form of Eq. 1 less sensitive to high noise levels of $C_T(t)$ was used to determine DVR and b:

$$\int_0^t C_T(\tau)d\tau = \mathrm{DVR}\left(\int_0^t C_R(\tau)d\tau + C_R(t)/\overline{k_2'}\right) + b\cdot C_T(t) \qquad (2)$$

When the ratio $C_R(t)$ to $C_T(t)$ is small or reasonably constant, the DVR can be obtained without the use of $\overline{k_2'}$, i.e.,

$$\frac{\int_0^t C_T(\tau)d\tau}{C_T(t)} = \mathrm{DVR}\frac{\int_0^t C_R(\tau)d\tau}{C_T(t)} + b' \qquad (3)$$

where $b' = \left(\mathrm{DVR}/\overline{k_2'}\right)(C_R(t)/C_T(t)) + b$.

Simplified reference tissue model

Assuming that the exchange rates between the nondisplaceable and specific compartments are rapid so that they can be combined into a single compartment and that both reference and target regions have the same level of nondisplaceable binding, the kinetics in the target region can be described by a simplified reference tissue model (SRTM) [18], using a reference region virtually devoid of specific binding as an input function. Defining R_1 (unitless) as the ratio of delivery (or perfusion) in the target tissue to that in the reference region, the target tissue TAC can be fitted by a slightly modified SRTM equation:

$$C_T(t) = R_1\left[C_R(t) + k_2'\left(1 - \frac{R_1}{\mathrm{DVR}}\right)C_R(t) \otimes \exp\left(-\frac{R_1 k_2'}{\mathrm{DVR}}t\right)\right] \qquad (4)$$

where $\otimes$ denotes the convolution operator, and R_1, k_2' and DVR can be estimated using the nonlinear least-squares Levenberg-Marquardt minimization algorithm [19].

Relative perfusion from early time data

By normalizing each voxel in the summed image of the first 6 min of dynamic image data by the sum of data within the same time interval in the reference region, tissue perfusion (R_p) relative to the reference region can be estimated as:

$$R_p = \frac{\int_{0\,\mathrm{min}}^{6\,\mathrm{min}} C_T(\tau)\mathrm{d}\tau}{\int_{0\,\mathrm{min}}^{6\,\mathrm{min}} C_R(\tau)\mathrm{d}\tau}, \qquad (5)$$

which serves as an approximation of regional delivery relative to the reference region. Regional relative perfusion can be obtained by calculating the values within the ROIs superimposed on the R_p image. Using different reference regions, the choice of a time interval of 0–6 min to generate R_p estimates has been found to be optimal based on their variability and their goodness-of-fit against R_1 estimates obtained with SRTM for control subjects and AD patients separately (see Results).

Data analysis

Logan graphical analysis and model fits were performed with programs developed in-house written in C++ and MATLAB (The MathWorks, Natick, MA). Statistical analyses were performed using SPSS 16.0 for Windows (SPSS, Chicago, IL). The results are presented as the mean±1SD unless otherwise stated. A p-value <0.05 was considered statistically significant.

Determination of efflux rate constant and regional DVR estimates

Theoretically, there should be only one value of k_2' as there is only one reference region. A different value of k_2' is estimated for different target tissues by SRTM and the variability of k_2' could be large. It has been suggested that a median value of k_2' estimated for all voxels/ROIs outside the reference region by SRTM should be used to re-estimate R_1 and the binding potential [20]. To reduce variability and improve parameter estimation, a modeling approach [21] equivalent to maximum-likelihood estimation was applied to fit all target tissue TACs simultaneously with SRTM (SIME-SRTM) by taking advantage of the fact that k_2' is the same across all target regions [6]. It has been shown that fixing k_2' in SRTM provides significantly better results than without fixing it [6, 7]. The median value of k_2' estimates obtained by SIME-SRTM for each study group was used as the population-averaged $\overline{k_2'}$ in the Logan analysis to determine regional DVR values for subjects in the same group. The standard error (SE) of the median estimate of k_2' was calculated using median absolute deviation [22]. For comparison, median values and SEs of k_2' computed using individual SRTM fits for both groups were also determined. The use of a simpler form of Logan analysis (Eq. 3) was also investigated.

Group comparisons

Regional R_p, R_1, and DVR values were calculated as a volume-weighted average of left and right regions. Global values of R_p, R_1, and DVR for each individual were calculated as their corresponding mean values of posterior cingulate, frontal, parietal, medial temporal, and lateral temporal cortices. Correspondences between R_p and R_1, and DVR estimates obtained by the Logan method, SRTM and SIME-SRTM were evaluated by linear regression analysis. Group differences were examined using a nonparametric Mann-Whitney rank-sum test. The Kruskal-Wallis test with Dunn's post test was used to compare differences in regional perfusion relative to white matter obtained with SRTM in control subjects and AD patients.

Stability of Logan DVR estimates

Logan analysis requires the definition of a time (t^*) beyond which the linearity of the plot is assured. Identification of this time is usually based on visual inspection. Bias and variability of regional DVR estimates due to different choices of t^* were assessed by progressively increasing t^* from 15 min to 85 min. The relationship between regional DVR estimates and total scan duration was examined by truncating brain datasets gradually from 0–125 min to 0–65 min. The relationship between $\overline{k_2'}$ and DVR estimates was evaluated by varying $\overline{k_2'}$ from −80% to +100% above its population value. The DVR estimates obtained with shortened total scan durations, increasing t^* and varying $\overline{k_2'}$ were compared with the reference values obtained using the complete 125-min datasets with t^*=35 min and $\overline{k_2'}$ at its population value determined by SIME-SRTM. The estimates were considered stable if the result was within ±5% of that from the reference values and the coefficient of variation (CV) less than 10%.

Discriminant analysis

To compare the classification and prediction performance in discriminating control subjects from AD patients using either the subcortical white matter or the cerebellum as the reference region, discriminant analysis [23] was conducted on the DVR estimates of the posterior cingulate, frontal, parietal, medial temporal, and lateral temporal cortices (which are the regions known to be affected by amyloid deposition) as predictor variables. The performance of discriminant analysis was evaluated with different combinations of regional DVR estimates as predictor variables and the chi-squared (χ^2) test was used to examine the overall accuracy in classification and prediction of group membership using the discriminant functions [23]. To estimate an unbiased and generalized performance measure for correct classification of new cases, cross-validation using a leave-one-out procedure was applied where each case was classified by the discriminant function derived from all cases other than that case.

Results

Clinical and cognitive measures

There were no differences between the groups in terms of age or gender. The MMSE scores of the AD patients were significantly lower than those of the control subjects (p<0.001).

[^{18}F]FDDNP kinetics

Representative regional tissue TACs obtained from a control subject and an AD patient are shown in Fig. 1a and d, respectively. Slower wash-in and clearance of [^{18}F]FDDNP was seen in the subcortical white matter, whereas the wash-in and clearance in the cerebellum was much faster and comparable with other cortical regions. The target-to-reference ratio became relatively constant at approximately 25 min following [^{18}F]FDDNP injection when the cerebellum was used as the reference region

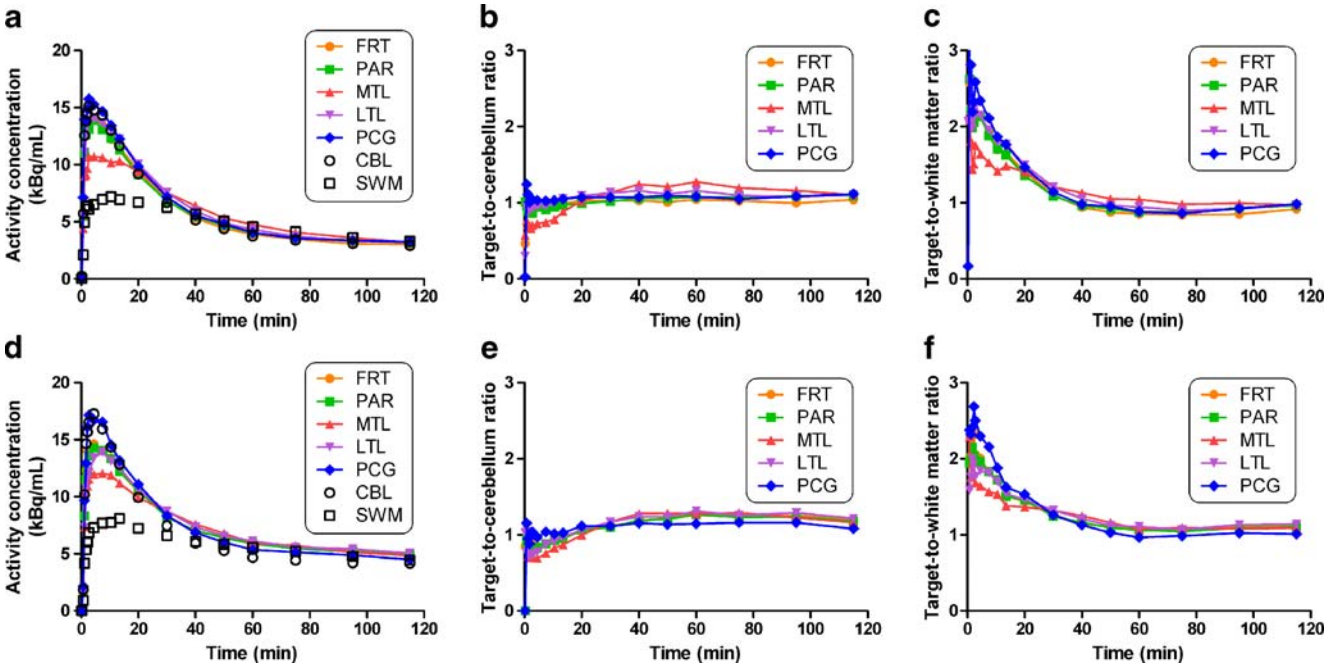

Fig. 1 Representative tissue TACs of a control subject (**a**) and an AD patient (**d**), and their ratios to the cerebellum (**b**, **e**) and white matter (**c**, **f**) (*FRT* frontal, *PAR* parietal, *MTL* medial temporal, *LTL* lateral temporal, *PCG* posterior cingulate, *CBL* cerebellum, *SWM* subcortical white matter)

(Fig. 1b and e). However, this ratio continued to decrease and became relatively constant at only about 60 min after injection when the white matter was used as the reference region (Fig. 1c and f).

Perfusion relative to the reference region

The optimal time interval was investigated independently in control subjects and AD patients using different reference regions (i.e., subcortical white matter and cerebellum) for calculating the relative perfusion (R_p) from the early summed image. The time intervals used were 0–0.5, 0–1, 0–1.5, 0–2, 0–2.5, 0–3, 0–6, 0–9, and 0–12 min after injection. Regional R_p estimates obtained with different time intervals were compared with R_1 estimates derived by SRTM. The CV of R_p estimates was generally increased when the interval was too short (<3 min) or too long (>6 min), whereas time interval 0–6 min provided R_p estimates with CV comparable to that of R_1 for both study groups and different reference regions. Linear regression analysis showed that R_p estimates obtained with 0–6 min were in good agreement with R_1, yielding the largest r^2 and lowest standard deviation of residuals amongst all time intervals used, regardless of which study group and reference region were investigated. Therefore, the optimal time interval for calculation of R_p was determined as 0–6 min after injection, based on our scanning protocol.

Figure 2 shows the scatter plots of relative perfusion calculated from the summed image data (R_p) within the first 6 min after injection of [^{18}F]FDDNP and from the SRTM (R_1) in various regions, using white matter and cerebellum as reference regions. The R_p estimates of perfusion relative to white matter and cerebellum were about 20% and 13% lower than the R_1 estimates obtained by SRTM. However, there was a strong correlation (r>0.97) between R_p and R_1 estimates in both the control and AD groups. Regional and global R_1 estimates obtained with SRTM using the white matter as the reference region are summarized in Table 1. No significant differences were observed in regional and global R_1 values between control subjects and AD patients but the difference among regions was statistically significant (Kruskal-Wallis test, p<0.0001). Dunn's post test revealed that there were significant differences in the medial temporal region (in both groups) as compared to the posterior cingulate in both groups (p<0.01) and to the frontal region in AD patients (p<0.05). Similar results were obtained for SIME-SRTM (data not shown).

Determination of population efflux rate constant

Variability of median estimate (in terms of CV) of k_2' derived by SRTM was 20±7% in white matter and 73±20% in cerebellum for control subjects, and 24±8% in white matter and 46±14% in cerebellum for AD patients. Improved estimates were obtained for k_2' by SIME-SRTM as the variability was reduced tremendously in both control subjects (2.1±0.4% for white matter and 6.7±1.1% for cerebellum) and AD patients (2.2±0.4% for white matter

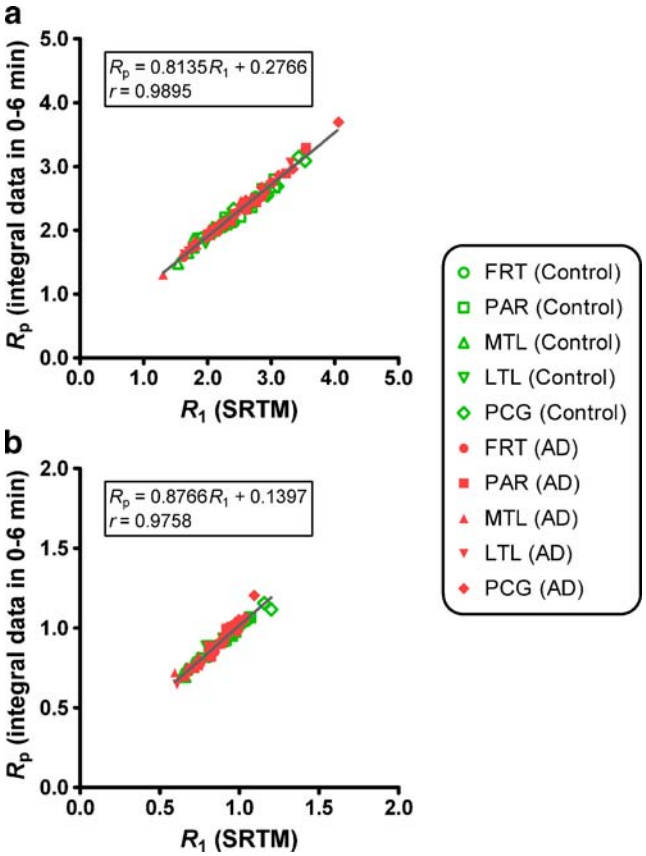

Fig. 2 Correlations between estimates of relative perfusion (to the reference region) using the summed image data (R_p) within the first 6 min after injection of [^{18}F]FDDNP, and perfusion (relative to the reference region) obtained by SRTM (R_1) for various regions in control subjects and AD patients. The reference regions were white matter (**a**) and cerebellum (**b**). Regression lines are shown in gray (*FRT* frontal, *PAR* parietal, *MTL* medial temporal, *LTL* lateral temporal, *PCG* posterior cingulate)

and 5.8±1.4% for cerebellum). The population estimates (median±SE) of k_2' (i.e., $\overline{k_2'}$) in white matter derived by SIME-SRTM were 0.023±0.005 min^{-1} and 0.023±0.004 min^{-1} for control subjects and AD patients, respectively, and did not differ significantly. Variability of $\overline{k_2'}$ determined by SIME-SRTM in white matter was similar to that in cerebellum, whose estimates (median±SE) of $\overline{k_2'}$ were 0.091±0.014 min^{-1} and 0.086±0.021 min^{-1} for control subjects and AD patients, respectively. These estimates were not significantly different from those obtained by SRTM.

Nonspecific binding

Figure 3 shows the Logan plots on the frontal cortex for a control subject without specific binding and in a typical AD patient using, respectively, the cerebellum and the subcortical white matter as reference region. The DVR values obtained with either reference region were identical for the control subject and were only slightly lower for the AD patient when the subcortical white matter was used as the reference region. To further demonstrate the similarity in nonspecific binding between the cerebellum and the subcortical white matter, Logan analysis was performed using, respectively, the subcortical white matter and the cerebellum as reference region. Representative results are shown in Fig. 4 for the same subjects shown in Fig. 3. The DVR values obtained for subcortical white matter and the cerebellum using their counterpart as reference region were very close to unity (1.02±0.04 and 0.98±0.05 for control subjects; 1.04±0.03 and 0.96±0.03 for AD patients), indicating that the levels of nonspecific binding in these regions were very similar.

Logan DVR with reference tissue input

Parametric DVR images using the white matter as the reference region for a control subject and an AD patient are shown in Fig. 5. The images were generated by applying Logan analysis on a voxel-by-voxel basis to dynamic PET images using data from 0–125 min (t^*=35 min). Binding of [^{18}F]FDDNP in the medial temporal, lateral temporal, posterior cingulate, parietal, and frontal regions was much more prominent in the AD patient than in the control subject. Regional DVR values obtained by Logan analysis using different reference regions are shown in Fig. 6. The regional and global DVR values were significantly higher in AD patients in comparison with control subjects. In both study groups, the rank order for DVR estimates was: medial temporal region > posterior cingulate > lateral temporal region > parietal region > frontal region. The same rank order was also observed for DVR estimates obtained with

Table 1 Regional R_1 obtained with SRTM using subcortical white matter as reference region. Values are mean±SD

Group[a]	Frontal	Parietal	Medial temporal	Lateral temporal	Posterior cingulate	Global
Control	2.42±0.32	2.61±0.33	1.86±0.22	2.32±0.34	2.97±0.42	2.44±0.31
AD	2.62±0.49	2.51±0.51	1.97±0.30	2.33±0.46	2.84±0.57	2.45±0.45

p<0.05, Medial temporal/Control vs Frontal/AD, and Medial temporal/AD vs Frontal/AD; p<0.01, Medial temporal vs Posterior cingulate, in both the control and AD groups; Dunn's post test.

[a] No significant difference was observed between the control and AD groups, but there were significant differences across regions (Kruskal-Wallis test, p<0.0001).

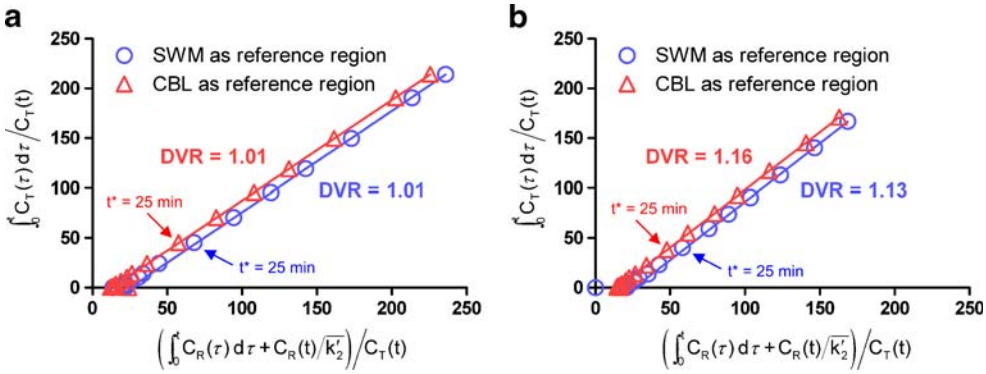

Fig. 3 Logan DVR plots on the frontal cortex for a control subject (**a**) and an AD patient (**b**) using the cerebellum (*CBL*) and the subcortical white matter (*SWM*) as reference region, respectively. The value of k_2' was 0.023 min^{-1} when SWM was used as the reference region and it was 0.091 min^{-1} for the control subject and 0.086 min^{-1} for the AD patient when CBL was used as the reference region. Note the similarity in DVR values derived using either reference region. The time point corresponding to the "pseudo" equilibrium (t^*=25 min) is also shown

SRTM and SIME-SRTM (data not shown). Regional DVR values obtained using either reference region were related by $DVR_{[white\ matter\ as\ reference\ region]}=0.96\ DVR_{[cerebellum\ as\ reference\ region]}$ (r=0.81, p<0.0001). This linear relation can be derived from the ratio of the specific binding to the nondisplaceable binding using different reference regions (see Appendix).

The DVR estimates obtained with either SRTM or SIME-SRTM using white matter as reference region were in good agreement with those derived by the Logan method ($DVR_{[SRTM]}=0.97\ DVR_{[Logan]}+0.02$, r=0.96, p<0.0001; $DVR_{[SIME\text{-}SRTM]}=1.04\ DVR_{[Logan]}-0.06$, r=0.95, p<0.0001). Neither the slopes nor the intercepts of the regression lines differed significantly from one or zero, respectively (extra sum-of-squares F-test, p>0.05).

Time stability of Logan DVR

Figure 7 shows the effect of t^* on the accuracy of Logan DVR in control subjects and AD patients with complete datasets (0–125 min). The bias in DVR values due to increasing t^* from 15 min to 85 min was calculated using estimates obtained with t^*=35 min as reference and was slightly larger in control subjects than in AD patients. The variability of regional DVRs obtained with t^* between 15 min and 65 min was similar to those obtained with t^*=35 min, but increased appreciably when t^*>65 min, especially in the posterior cingulate. The maximum allowable t^* was found to be 45 min without introducing significant bias and variability to the DVR estimates.

Figure 8 shows the effect of total scan duration on the accuracy of regional DVR estimates derived by Logan analysis in control subjects and AD patients with t^*=35 min. When the total scan duration was shortened from 125 min to 65 min, the DVR estimates and the variability in all regions steadily decreased and increased, respectively. However, less than 5% changes were observed for regional DVR estimates and the CV was less than 10% even though the total scan duration was shortened to 65 min.

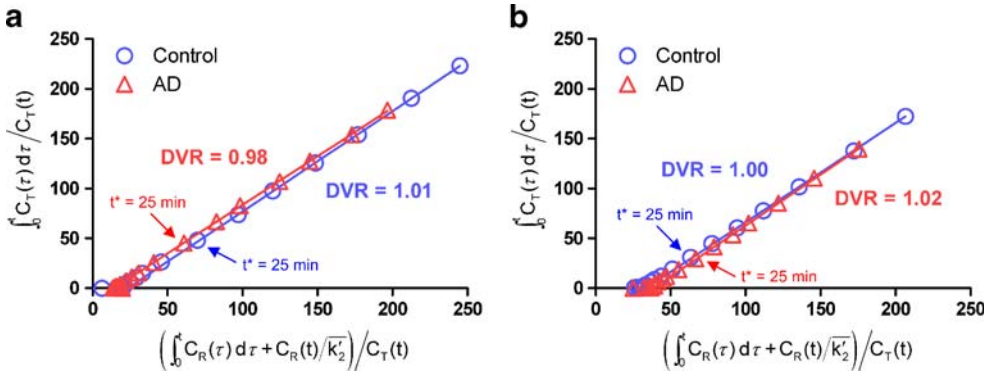

Fig. 4 Logan DVR plot on the cerebellum using the subcortical white matter as reference region (**a**) and the subcortical white matter using the cerebellum as reference region (**b**) for the same subjects as shown in Fig. 3. The time point corresponding to the "pseudo" equilibrium (t^*=25 min) is also shown

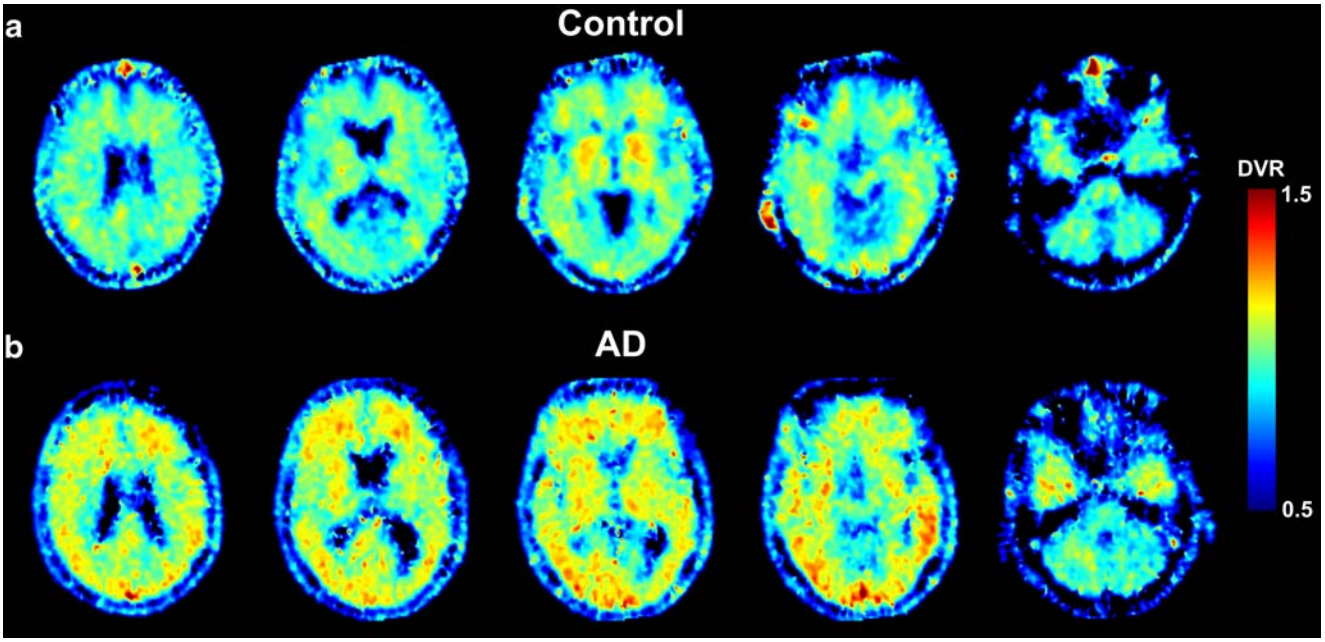

Fig. 5 Representative parametric images of Logan DVR using 125 min of data (with t^*=35 min) and white matter as reference input in a control subject (**a**) and an AD patient (**b**)

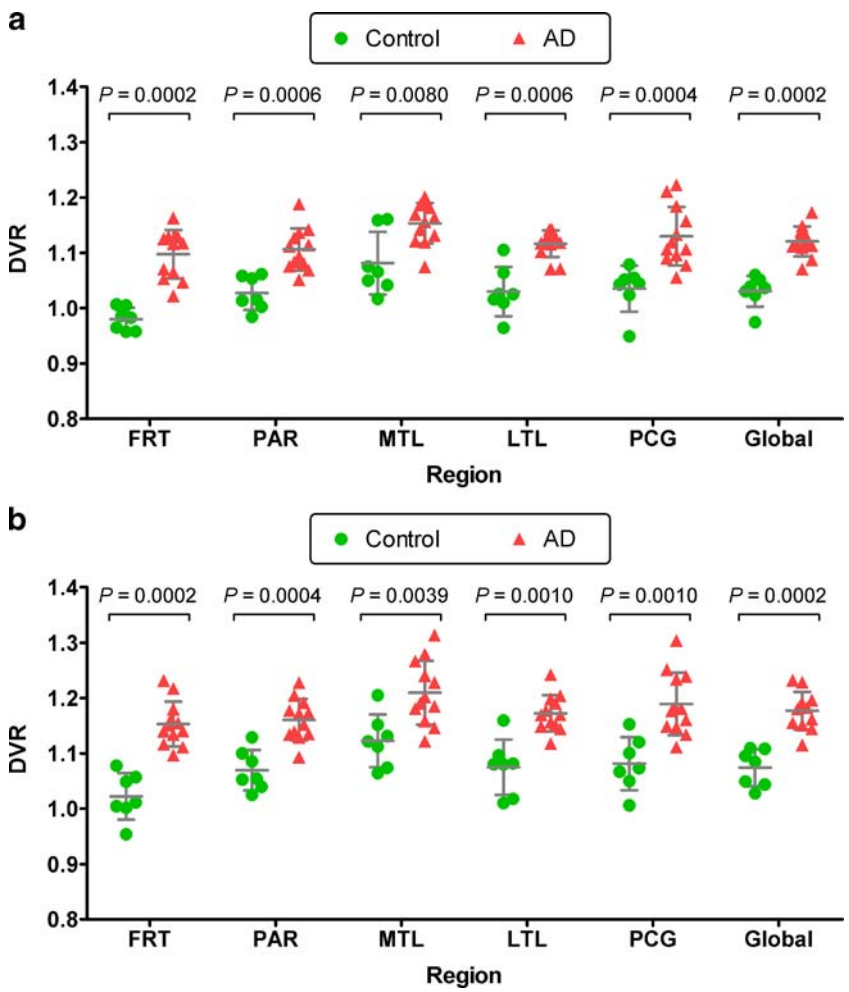

Fig. 6 Scatter plots of regional [^{18}F]FDDNP binding derived by the Logan method using white matter (**a**) and cerebellum (**b**) as reference regions. Long and short horizontal bars represent means and standard deviations, respectively. The *p*-values were calculated using a nonparametric Mann-Whitney rank-sum test (one-tailed)

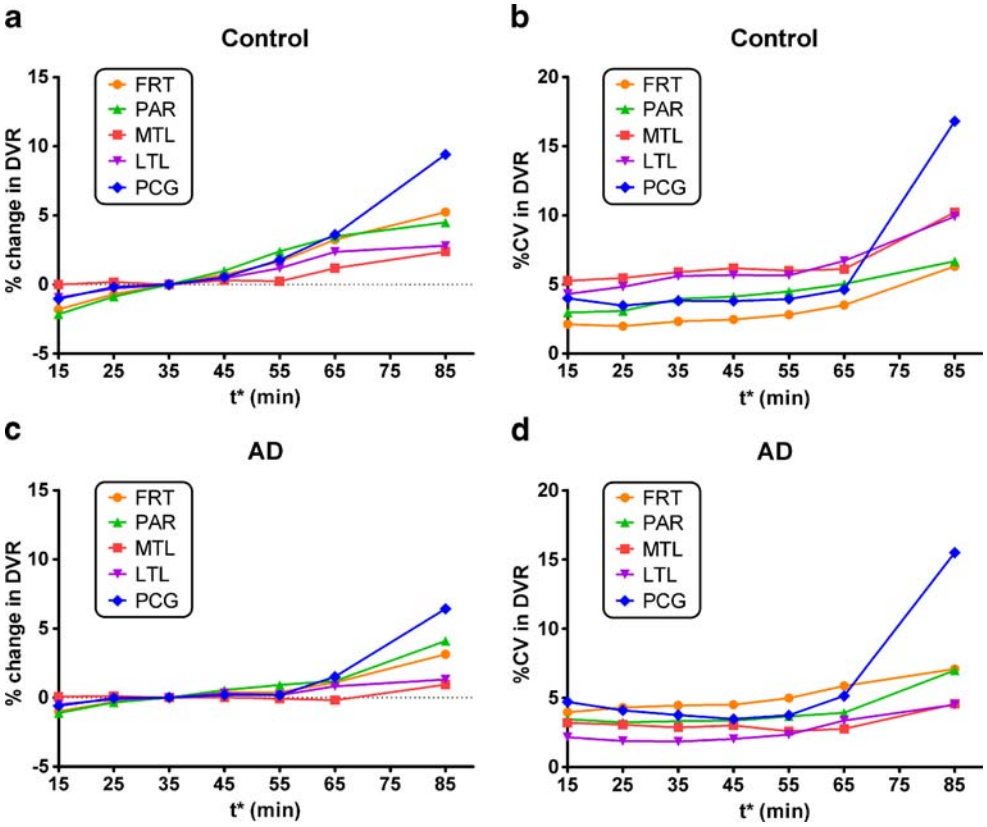

Fig. 7 Effect of varying t^* on the stability of regional DVR values derived by the Logan method with subcortical white matter as reference region in control subjects and AD patients for each region (n=5) and each subject (n=7 control subjects, n=12 AD patients). Percentage differences in DVR values due to increasing t^* from 15 min to 85 min were calculated using estimates obtained with t^*=35 min as reference values and are shown for control subjects (**a**) and AD patients (**c**), and the corresponding variability is shown for control subjects (**b**) and AD patients (**d**)

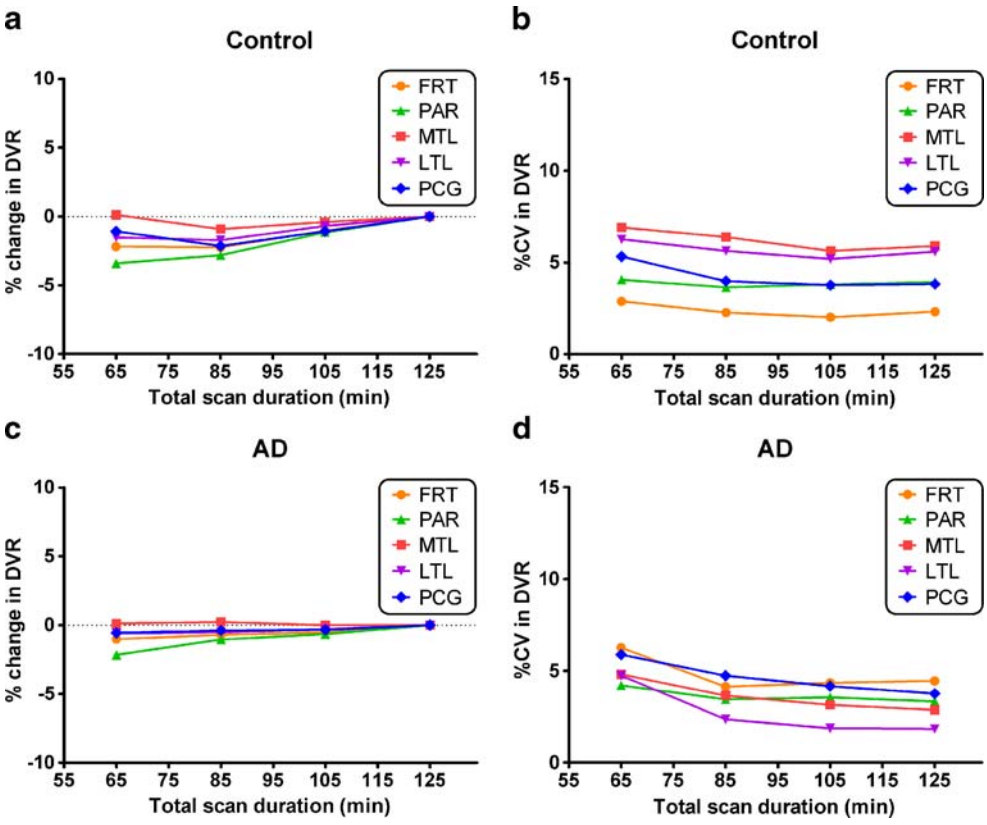

Fig. 8 Effect of total scan duration on the stability of regional DVR values derived by the Logan method with subcortical white matter as reference region in control subjects and AD patients for each region (n=5) and each subject (n=7 control subjects, n=12 AD patients). Regional DVR values derived with shorter datasets, expressed as a percentage difference from their reference values estimated with the complete datasets (125 min of data collection and t^*=35 min) are shown for control subjects (**a**) and AD patients (**c**). The variability, expressed as %CV, is shown for control subjects (**b**) and AD patients (**d**)

Effect of efflux rate constant on Logan DVR

Figure 9 shows the effect of the value of $\overline{k_2'}$ on the accuracy of DVRs derived by Logan analysis. All regions exhibited a similarly large dependence on the value of $\overline{k_2'}$ in both control subjects and AD patients. Varying the value of $\overline{k_2'}$ from −80% to +100% above the population value of 0.023 min^{-1} resulted in variations in the regional DVR values varied from −19.7% to +3.1% in control subjects (Fig. 9a) and from −21.2% to +3.4% in AD patients (Fig. 9b) over their means and the DVR values were more susceptible to negative bias in the $\overline{k_2'}$ value. Increasing $\overline{k_2'}$ tenfold (which covered a wide range of plausible values) or eliminating the term $\overline{k_2'}$ from the calculation of DVR resulted in a variation ranging from +1.5% to +7.1% in all regions examined.

Discriminant analysis

Table 2 summarizes the classification accuracy, sensitivity and specificity of discriminant analysis using different combinations of regional DVR estimates as predictor variables. The classification performance was generally improved when more predictor variables were included in the discriminant analysis. There was an excellent discrimination between control subjects and AD patients, with 100% classification accuracy using either the white matter ($\chi^2_{(5)} = 27.3$, $p<0.001$) or the cerebellum ($\chi^2_{(5)} = 22.4$, $p<0.001$) as the reference region when the discriminant analysis conducted on the Logan DVR estimates of the posterior cingulate, and frontal, parietal, medial temporal, and lateral temporal regions with complete datasets (0–125 min). The leave-one-out cross-validation procedure yielded 92% sensitivity and 100% specificity, with an overall accuracy of 95% for using either reference region.

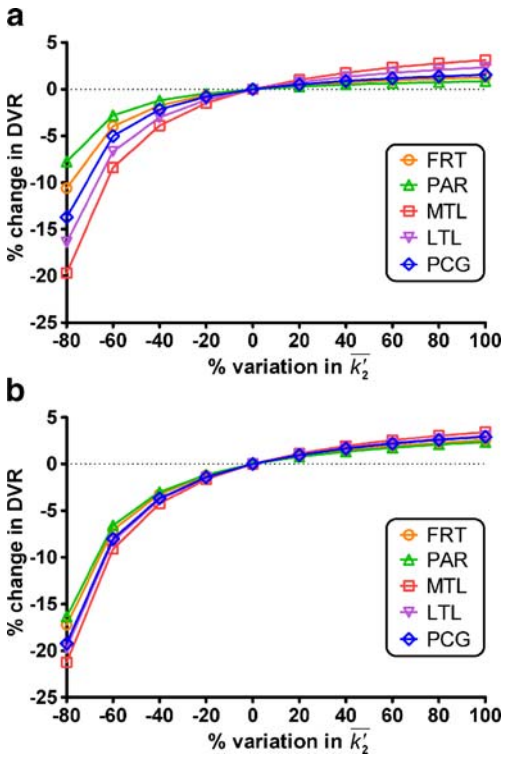

Fig. 9 Effect of variation in $\overline{k_2'}$ in white matter on the accuracy of DVRs derived by Logan graphical analysis in control subjects (**a**) and AD patients (**b**). Variations in DVR in the frontal region (*FRT*), parietal region (*PAR*), medial temporal region (*MTL*), lateral temporal region (*LTL*), and posterior cingulate (*PCG*) were determined using an assumed $\overline{k_2'}$ value of 0.023 min^{-1}

Discussion

The primary aims of this study were to evaluate the use of the subcortical white matter as a reference region and to determine whether it is a good alternative to the cerebellum, which could be affected by disease. It is an important issue that is not only specific to [^{18}F]FDDNP for amyloid imaging but also relevant to generic neuroreceptor studies when no appropriate cortical region can be used as reference tissue due to the presence of specific binding. Post-mortem studies have shown that amyloid deposition in the white matter is much less than in most cortical regions and the cerebellum. The most important finding in this study is that regional DVRs obtained with the white matter as the reference region possess the same distinguishing ability as those obtained with the cerebellum, and show significant differences between control subjects and AD patients. The regional binding of [^{18}F]FDDNP agrees well with topographical patterns of pathological distribution seen at autopsy [13, 24, 25]. In this regard, the subcortical white matter may be an adequate alternative reference region to the cerebellum when the latter is affected by the pathology of the disease. A typical example is in prion disease such as GSS syndrome whose pathological hallmark is the presence of numerous mutant prion protein amyloid deposits throughout the cerebral cortices, especially in the cerebellum [12], where [^{18}F]FDDNP binding has been found to be elevated [3].

Recent studies [6, 7] have demonstrated that the full reference tissue model [26] provides less reliable fits to regional [^{18}F]FDDNP kinetics than SRTM. Therefore, only SRTM was considered in this study and the results were compared with those from the Logan method. While SRTM provides more kinetics information such as transport, efflux and binding, it has more stringent requirements than Logan analysis that need to be satisfied. In addition to assuming that the reference region contains no or negligible specific binding, the kinetics in both target and reference regions need to be adequately described by a one-tissue compartment model [18]. If this latter assumption is violated,

Table 2 Classification accuracy, sensitivity, and specificity (%) using regional Logan DVR values derived with subcortical white matter and cerebellum as reference input

Regions	Reference region					
	Subcortical white matter			Cerebellum		
	Accuracy	Sensitivity	Specificity	Accuracy	Sensitivity	Specificity
FRT+PAR+MTL+LTL+PCG	100 (95)	100 (92)	100 (100)	100 (95)	100 (92)	100 (100)
FRT+MTL+LTL+PCG	100 (95)	100 (92)	100 (100)	100 (95)	100 (92)	100 (100)
PAR+FRT+MTL+PCG	100 (95)	100 (92)	100 (100)	100 (95)	100 (92)	100 (100)
FRT+MTL+LTL	100 (95)	100 (92)	100 (100)	100 (95)	100 (92)	100 (100)
FRT+MTL+PCG	100 (95)	100 (92)	100 (100)	100 (95)	100 (92)	100 (100)
MTL+LTL+PCG	90 (90)	92 (92)	86 (86)	95 (90)	100 (92)	86 (86)
PCG+PAR	95 (90)	92 (83)	100 (100)	90 (90)	92 (92)	86 (86)
PCG+LTL	95 (90)	100 (92)	86 (86)	90 (90)	92 (92)	86 (86)
PAR+LTL	90 (90)	92 (92)	86 (86)	90 (84)	92 (92)	86 (71)

Cross-validated values are given in parentheses.

FRT frontal, *PAR* parietal, *MTL* medial temporal, *LTL* lateral temporal, *PCG* posterior cingulate.

independent of the presence of specific binding in the reference region, the DVR estimates obtained by SRTM will be biased [20]. This assumption was checked using the same model evaluation strategies adopted by Wong et al. [6], and it was found that SRTM outperformed the full reference tissue model in 85% of model fits using the white matter as the reference region (data not shown). This finding is in line with the findings of our previous study [6] and that by Yaqub et al. [8] who concluded that, although it might not be ideal, SRTM is the method of choice for quantitative analysis of [^{18}F]FDDNP data. On the contrary, although Logan analysis might not be ideal, the good correspondence with SRTM as indicated by our results and those of Yaqub et al. [7], and the robustness and computational ease of Logan analysis would make this approach practical and attractive for routine parametric mapping of amyloid and tau deposition with [^{18}F]FDDNP PET.

Due to different composition of gray matter and white matter, it is likely that the nonspecific binding in these regions would not be the same. However, their ratio should be quite constant. Our data showed that the nonspecific binding of [^{18}F]FDDNP in these regions was quite similar and was close to 1 (Figs. 3 and 4). The slight difference in nonspecific binding between the cerebellum and the subcortical white matter caused a slight but constant DVR bias (lowered by about 5%) in all gray matter target regions over subjects and groups when using the white matter rather than the cerebellum as reference region. However, this may not be true for other amyloid imaging probes such as [^{11}C]PIB and [^{18}F]BAY94-9172 as indicated by the large DVR values in the subcortical white matter with cerebellum as reference region (control subjects 1.33±0.06, AD patients 1.34±0.18 for [^{11}C]PIB [27]; control subjects 1.93±0.18, AD patients 1.89±0.45 for [^{18}F]BAY94-9172 [28]), and thus these probes will need to be carefully investigated. The same is also true, and perhaps even more important, for neuroreceptor studies, as in that case it is more likely that nonspecific binding could be different between gray matter and white matter.

The hydrophobic nature of [^{18}F]FDDNP makes it highly permeable through the blood–brain barrier. Delivery of the tracer from blood to tissue is mostly perfusion-limited and the vascular volume, for all practical purposes, can be considered as part of the tissue compartment of free [^{18}F]FDDNP. Therefore, the effect of blood volume on the estimate of relative perfusion or K_1 is expected to be relatively small. The initial image data obtained immediately after injection of [^{18}F]FDDNP thus mainly reflects perfusion-dependent activity distributions. Relative perfusion (to the reference region) could be obtained by normalizing regional perfusion with that in the reference region. Perfusion estimates obtained by this approach (R_p) were slightly lower than but highly correlated with those (R_1) derived by SRTM (Fig. 2).

While the forward transport of [^{18}F]FDDNP is flow-dependent and the difference in perfusion between gray matter and white matter is much larger than it is between gray matter regions where reference tissue models are usually applied, a slowly perfused (reference) region would simply indicate that a longer time is required for tracer delivery and for reaching a "steady-state" equilibrium, and thus a longer t^* is needed to derive Logan DVR. This is problematic for compounds with short half-lives but not so

for ^{18}F-labeled compounds, which typically have a longer data acquisition time. Since DVR represents equilibrium binding quantity and as such is independent of blood flow [9, 29]. Our data suggest that a "pseudo" equilibrium condition is typically reached by 25 min after injection (Figs. 3 and 4) even though "steady-state" equilibrium is not yet attained and the calculated DVR values were quite stable (Figs. 7 and 8). Therefore, providing that the blood flow is reasonably stable during the period of study, differences in blood flow between gray matter and white matter do not limit the use of white matter as a reference region. Consequently, elevated regional DVR seen in AD patients as compared to control subjects should not be due to decreased perfusion. This argument was supported by the observations that there was no significant difference in regional relative delivery between control subjects and AD patients (Table 1) and that the rank order of DVR values (Fig. 6) was consistent with the typical rank order of amyloid deposits found in post-mortem AD brains [13, 24, 25].

The use of the reference tissue approach requires that R_1 is relatively constant across different brain regions [30]. Our results showed that this requirement was well satisfied, as R_1 values were very similar across regions, except in the medial temporal region, where lower R_1 values were observed in both groups (Table 1), likely due to various confounding factors, including partial volume effect and the reconstruction algorithm used. The relatively small size of the medial temporal region also makes it prone to higher anatomic variability with aging and degeneration. It is worth mentioning that metabolic and perfusion studies have yielded conflicting results on the functional status of the medial temporal region in patients with AD [31, 32].

Although the efflux rate constant for a given population needs to be determined a priori, this work and also a recent study [7] indicate that regional [^{18}F]FDDNP binding is relatively insensitive to the value of the efflux rate constant chosen, and the efflux rate constants for normal control subjects and AD patients are similar for a given reference region. We expect that efflux rate constants for subjects with MCI or frontotemporal dementia would be similar to those of normal control subjects and AD patients.

The decreasing ratio of target ROI to white matter shown in Fig. 1 suggests that the determination of the Logan DVR is sensitive to the $C_R(t)/\overline{k_2'}$ term in Eqs. 1 and 2. Even though $C_T(t)/C_R(t)$ was relatively constant after 40 min, larger bias and variance were seen in DVR estimates derived with Eq. 3, particularly when the total scan duration was shortened (data not shown). Therefore, the use of the simpler form of Logan analysis is not recommended when white matter is used as the reference region. The dependence of the DVR estimates on the value of $\overline{k_2'}$ is shown in Fig. 9 for the frontal, parietal, medial temporal, lateral temporal and posterior cingulate regions. All regions exhibited a large dependence on the value of $\overline{k_2'}$ in both control subject and AD groups and were more susceptible to negative bias on $\overline{k_2'}$.

While there were significant differences in regional DVR between control subjects and AD patients, the degree of overlap between the groups was such that using a single DVR parameter in any region lacked sensitivity. Discriminant analysis provides an objective means to classify subjects by using multiple regional DVR parameters as predictor variables in conjunction with known group information. Considering DVR parameters of multiple regions simultaneously in discriminant analysis yielded highly accurate classification of control subjects and AD patients, and the results using the white matter or the cerebellum as the reference region were in very good agreement (Table 2). By using DVR parameters in five regions (frontal, parietal, medial temporal, lateral temporal, and posterior cingulate), excellent discrimination between control subjects and AD patients was achieved, with 100% sensitivity, specificity and classification accuracy (cross-validated 95%), using either reference regions (Table 2). There is a concern that retrospective selection of subjects is not the appropriate approach when the intent is discriminating AD patients from control subjects, especially when a predictive model is to be developed. However, it should be noted that the "diagnostic performance" results reported in Table 2 are not related to the retrospective selection of subjects. Instead, Table 2 was intended only to show comparisons of classification performance based on regional DVR parameters derived with different reference regions (i.e., subcortical white matter versus cerebellum) regardless of clinical diagnosis. It was demonstrated that both reference regions provided virtually identical results for overall accuracy, sensitivity, and specificity of classification.

In practice, it is not known in advance whether the cerebellum would be affected by disease if blood data are not available. However, due to its invasiveness, peripheral blood sampling is not practical in a clinical setting because it is laborious and may not be tolerated by the patient particularly when longitudinal evaluations are required. Despite the slight systematically lower DVR values obtained with subcortical white matter, it performed as well as the cerebellum as reference region in terms of overall subject classification accuracy and regional DVR comparisons between subject groups. Therefore, when blood data are not available or blood sampling is not feasible due to practical clinical considerations, both subcortical white matter and the cerebellum should be used together as a quality check to assess if there is any discrepancy in the results that may require further investigation along with other clinical information. On the other hand, the control subjects and AD patients included in this study were not patients with specific vascular abnormal-

ities, vascular dementia, or multiple sclerosis. For subjects with these diseases, the use of white matter as reference region would require further validation and careful investigation. Indeed, this is one of the subjects of our future research.

Conclusion

We evaluated the use of the subcortical white matter as the reference region for quantitative analysis of [^{18}F]FDDNP PET data and the results were compared with those using the cerebellum as the reference region. The use of the white matter as a reference region is possible with [^{18}F]FDDNP PET determinations because the steady-state ratio of white matter over cerebellum is constant and close to 1 (control subjects 1.02±0.04; AD patients 1.04±0.03). Our results suggest that Logan graphical analysis is a robust method to derive regional DVR parameters with low bias and variability and is independent of tracer delivery, but it shows dependence on the efflux rate constant in subcortical white matter that needs to be determined a priori (e.g., by model fitting with a physiological constraint). The rank order of DVR values derived using the white matter as the reference region agrees well with that using the cerebellum as the reference region and is consistent with the typical rank order of amyloid deposits seen at autopsy. The performance in classifying subjects by discriminant analysis using the subcortical white matter as the reference region was similar to that using the cerebellum as the reference region. Therefore, the subcortical white matter is a good alternative reference region to the cerebellum for analyzing [^{18}F]FDDNP PET data particularly when the latter region is affected by disease. In practice, both the subcortical white matter and the cerebellum should be used together to cross-validate the findings with different reference regions, especially when blood data are not available or blood sampling is not feasible due to practical clinical considerations.

Acknowledgments The authors thank Dr. Linda Ercoli for performing the neuropsychological tests; David Truong and Dat Vu for system and database support; UCLA Cyclotron staff for help with [^{18}F]FDDNP preparation and staff at the Division of Nuclear Medicine for technical assistance in PET imaging. This work was supported in part by the US Department of Energy (DOE contract DE-FG02-02ER63420) and NIH grant P01-AG025831. J.R.B. gratefully acknowledges the support of the Elizabeth and Thomas Plott Chair Endowment in Gerontology.

Conflicts of interest The University of California, Los Angeles, owns US patent (6,274,119) entitled "Methods for Labeling β-Amyloid Plaques and Neurofibrillary Tangles" that uses the approach outlined in this article and which has been licensed to Siemens. N.S., G.W.S., J.R.B., and S.C.H. are among the inventors, have received royalties, and may receive royalties on future sales. G.W.S. reports having served as a consultant and/or having received lecture fees from Abbott, Brainstorming Co., Dakim, Eisai, Forest, Medivation, Myriad Genetics, Novartis, Ortho-McNeil, Pfizer, Radica, and Siemens. G.W.S. also reports having received stock options from Dakim. J.R.B. reports having served as a consultant and having received lecture fees from Nihon Medi-Physics Co., Bristol-Meyer Squibb, PETNet Pharmaceuticals, and Siemens. S.C.H. reports having received lecture fees from GlaxoSmithKline. K.P.W., M.W., W.S., M.D., V.K., and J.L. declare no financial conflicts of interest.

Appendix

Theoretically, the relation between the regional DVR values obtained using either reference region can be derived from the ratio of the specific binding (V_T–V_{ND}) to the nondisplaceable binding (V_{ND}), i.e.,

$$BP_{ND} \equiv \frac{V_T - V_{ND}}{V_{ND}} = \frac{V_T}{V_{ND}} - 1 \tag{A1}$$

where V_T and V_{ND} represent the total distribution volume (DV) and nondisplaceable DV, respectively [33]. The latter parameter can be measured as V_T in a reference region. Denote $V_{ND(CBL)}$ and $V_{ND(SWM)}$ as the nondisplaceable (or total) DVs of the cerebellum (CBL) and the subcortical white matter (SWM), respectively. It is likely that $V_{ND(CBL)}$ and $V_{ND(SWM)}$ would not be the same but their ratio should be constant and is related by $V_{ND(CBL)}/V_{ND(SWM)} = c$, where c is a constant. For a target region with V_T as the total DV, if the cerebellum is used as the reference region, then from Eq. A1:

$$BP_{ND(CBL)} = \frac{V_T}{V_{ND(CBL)}} - 1 \equiv \frac{V_T}{c \cdot V_{ND(SWM)}} - 1 \tag{A2}$$

Similarly, if the subcortical white matter is used as reference region, then

$$BP_{ND(SWM)} = \frac{V_T}{V_{ND(SWM)}} - 1 \tag{A3}$$

Denote $DVR_{CBL} \equiv V_T/V_{ND(CBL)} = BP_{ND(CBL)} + 1$ and $DVR_{SWM} \equiv V_T/V_{ND(SWM)} = BP_{ND(SWM)} + 1$ as the DVR values obtained using the cerebellum and the subcortical white matter as reference region, respectively. Substituting DVR_{CBL}, DVR_{SWM} and Eq. A3 into Eq. A2 and rearranging, we have:

$$DVR_{CBL} = c' \cdot DVR_{SWM} \tag{A4}$$

or

$$DVR_{SWM} = c \cdot DVR_{CBL} \tag{A5}$$

where $c' = 1/c$. Therefore, regional DVR values obtained with the subcortical white matter and the cerebellum can be compared and related by a constant, and their relationship can

be determined by additional measurements (e.g., from blocking and displacement studies) or by linear regression on the DVR values derived using either reference region.

References

1. Small GW, Kepe V, Ercoli LM, Siddarth P, Bookheimer SY, Miller KJ, et al. PET of brain amyloid and tau in mild cognitive impairment. N Engl J Med 2006;355:2652–63.
2. Shin J, Lee S-Y, Kim S-H, Kim Y-B, Cho S-J. Multitracer PET imaging of amyloid plaques and neurofibrillary tangles in Alzheimer's disease. Neuroimage 2008;43:236–44.
3. Kepe V, Ghetti B, Farlow M, Bresjanac M, Miller K, Huang S-C, et al. PET of brain prion protein amyloid in Gerstmann-Sträussler-Scheinker disease. Brain Pathol 2009; doi:10.1111/j.1750-3639.2009.00306.x.
4. Barrio JR, Huang S-C, Cole G, Satyamurthy N, Petric A, Phelps ME, et al. PET imaging of tangles and plaques in Alzheimer disease with a highly hydrophobic probe. J Labelled Comp Radiopharm 1999;42:S194–5.
5. Agdeppa ED, Kepe V, Liu J, Flores-Torres S, Satyamurthy N, Petric A, et al. Binding characteristics of radiofluorinated 6-dialkylamino-2-naphthylethylidene derivatives as positron emission tomography imaging probes for β-amyloid plaques in Alzheimer's disease. J Neurosci. 2001;21:RC189(1–5).
6. Wong K-P, Kepe V, Small GW, Satyamurthy N, Barrio JR, Huang S-C. Comparison of simplified methods for quantitative analysis of [18F]FDDNP PET data. IEEE Nuclear Science Symposium and Medical Imaging Conference Record. Honolulu, Hawaii; 2007. p. 3146–50.
7. Yaqub M, Tolboom N, Van Berckel BN, Scheltens P, Lammertsma AA, Boellaard R. Simplified parametric methods for [18F]FDDNP studies. Neuroimage. 2009; doi:10.1016/j.neuroimage.2009.07.046.
8. Yaqub M, Boellaard R, Van Berckel BNM, Tolboom N, Luurtsema G, Dijkstra AA, et al. Evaluation of tracer kinetic models for analysis of [18F]FDDNP studies. Mol Imaging Biol 2009;11:322–33.
9. Logan J, Fowler JS, Volkow ND, Wang GJ, Ding YS, Alexoff DL. Distribution volume ratios without blood sampling from graphical analysis of PET data. J Cereb Blood Flow Metab 1996;16:834–40.
10. Joachim CL, Morris JH, Selkoe DJ. Diffuse senile plaques occur commonly in the cerebellum in Alzheimer's disease. Am J Pathol 1989;135:309–19.
11. Yamaguchi H, Hirai S, Morimatsu M, Shoji M, Nakazato Y. Diffuse type of senile plaques in the cerebellum of Alzheimer-type dementia demonstrated by β protein immunostain. Acta Neuropathol 1989;77:314–9.
12. Masters CL, Gajdusek DC, Gibbs CJ. Creutzfeldt-Jakob disease virus isolation from the Gerstmann-Sträussler syndrome with an analysis of the various forms of amyloid plaque deposition in the virus-induced spongiform encephalopathies. Brain 1981;104:559–88.
13. Thal DR, Rüb U, Orantes M, Braak H. Phase of Aβ-deposition in the human brain and its relevance for the development of AD. Neurology 2002;58:1791–800.
14. Folstein MF, Folstein SE, McHugh PR. Mini-mental state: a practical method for grading the cognitive state of patients for the clinician. J Psychiat Res 1975;12:189–98.
15. McKhann G, Drachman D, Folstein M, Katzman R, Price D, Stadlan EM. Clinical diagnosis of Alzheimer's disease: report of the NINCDS-ADRDA Work Group under the auspices of the Department of Health and Human Services Task Force on Alzheimer's Disease. Neurology 1984;34:939–44.
16. Liu J, Kepe V, Žabjek A, Petric A, Padgett HC, Satyamurthy N, et al. High-yield, automated radiosynthesis of 2-(1-{6-[(2-[18F] fluoroethyl)(methyl)amino]-2-naphthyl}ethylidene)malononitrile ([18F]FDDNP) ready for animal or human administration. Mol Imaging Biol 2007;9:6–16.
17. Wong K-P, Wardak M, Shao W, Zhou Z, Dahlbom M, Smid L, et al. Movement correction of [18F]FDDNP PET studies for brain amyloid imaging. IEEE Nuclear Science Symposium and Medical Imaging Conference Record. Honolulu, Hawaii; 2007. p. 3974–7.
18. Lammertsma AA, Hume SP. Simplified reference tissue model for PET receptor studies. Neuroimage 1996;4:153–8.
19. Marquardt DW. An algorithm for least-squares estimation of nonlinear parameters. J Soc Indust Appl Math 1963;11:431–41.
20. Wu Y, Carson RE. Noise reduction in the simplified reference tissue model for neuroreceptor functional imaging. J Cereb Blood Flow Metab 2002;22:1440–52.
21. Wong K-P, Feng D, Meikle SR, Fulham MJ. Simultaneous estimation of physiological parameters and the input function – in vivo PET data. IEEE Trans Inform Technol Biomed 2001;5:67–76.
22. Huber PJ. Robust statistical procedures. 2nd ed. Philadelphia: Society for Industrial and Applied Mathematics; 1996.
23. Anderson TW. An introduction to multivariate statistical analysis. 2nd ed. New York: Wiley; 1984.
24. Braak H, Braak E. Neuropathological stageing of Alzheimer-related changes. Acta Neuropathol 1991;82:239–59.
25. Price JL, Morris JC. Tangles and plaques in nondemented aging and "preclinical" Alzheimer's disease. Ann Neurol 1999;45: 358–68.
26. Lammertsma AA, Bench CJ, Hume SP, Osman S, Gunn K, Brooks DJ, et al. Comparison of methods for analysis of clinical [11C] raclopride studies. J Cereb Blood Flow Metab 1996;16:42–52.
27. Lopresti BJ, Klunk WE, Mathis CA, Hoge JA, Ziolko SK, Lu X, et al. Simplified quantification of Pittsburgh Compound B amyloid imaging PET studies: a comparative analysis. J Nucl Med 2005;46:1959–72.
28. Rowe CC, Ackerman U, Browne W, Mulligan R, Pike KL, O'Keefe G, et al. Imaging of amyloid β in Alzheimer's disease with 18F-BAY94-9172, a novel PET tracer: proof of mechanism. Lancet Neurol 2008;7:129–35.
29. Logan J, Volkow ND, Fowler JS, Wang G-J, Dewey SL, MacGregor RR, et al. Effects of blood flow on [11C]raclopride binding in the brain: model simulations and kinetic analysis of PET data. J Cereb Blood Flow Metab 1994;14:995–1010.
30. Cunningham VJ, Lammertsma AA. Radioligand studies in brain: kinetic analysis of PET data. Med Chem Res 1994;5:79–96.
31. Minoshima S, Giordani B, Berent S, Frey KA, Foster NL, Kuhl DE. Metabolic reduction in the posterior cingulate cortex in very early Alzheimer's disease. Ann Neurol 1997;42:85–94.
32. Ishii K, Sasaki M, Yamaji S, Sakamoto S, Kitagaki H, Mori E. Paradoxical hippocampus perfusion in mild-to-moderate Alzheimer's disease. J Nucl Med 1998;39:293–8.
33. Huang S-C, Barrio JR, Phelps ME. Neuroreceptor assay with positron emission tomography: equilibrium versus dynamic approaches. J Cereb Blood Flow Metab 1986;6:515–21.